

2012-02-01

## Preparation and Rapid Analysis of Antibacterial Silver, Copper and Zinc Doped Sol–gel Surfaces

Brendan Duffy

*Technological University Dublin, [brendan.duffy@tudublin.ie](mailto:brendan.duffy@tudublin.ie)*

Swarna Jaiswal

*Technological University Dublin, [swarna.jaiswal@tudublin.ie](mailto:swarna.jaiswal@tudublin.ie)*

Patrick McHale

*Technological University Dublin, [patrick.mchale@tudublin.ie](mailto:patrick.mchale@tudublin.ie)*

Follow this and additional works at: <https://arrow.tudublin.ie/cenresart>



Part of the [Analytical Chemistry Commons](#), [Materials Chemistry Commons](#), and the [Polymer Chemistry Commons](#)

---

### Recommended Citation

S. Jaiswal, et al. (2012) Preparation and rapid analysis of antibacterial silver, copper and zinc doped sol–gel surfaces, *Colloids Surf. B: Biointerfaces* Jun 1;94:170-6 (2012), doi:10.1016/j.colsurfb.2012.01.035

This Article is brought to you for free and open access by the Crest: Centre for Research in Engineering Surface Technology at ARROW@TU Dublin. It has been accepted for inclusion in Articles by an authorized administrator of ARROW@TU Dublin. For more information, please contact [arrow.admin@tudublin.ie](mailto:arrow.admin@tudublin.ie), [aisling.coyne@tudublin.ie](mailto:aisling.coyne@tudublin.ie), [vera.kilshaw@tudublin.ie](mailto:vera.kilshaw@tudublin.ie).

Funder: DIT ABBEST



Contents lists available at [SciVerse ScienceDirect](http://SciVerse.ScienceDirect)

## Colloids and Surfaces B: Biointerfaces

journal homepage: [www.elsevier.com/locate/colsurfb](http://www.elsevier.com/locate/colsurfb)



# Preparation and rapid analysis of antibacterial silver, copper and zinc doped sol–gel surfaces

Swarna Jaiswal<sup>a,b</sup>, Patrick McHale<sup>b</sup>, Brendan Duffy<sup>a,\*</sup>

<sup>a</sup> Centre for Research in Engineering Surface Technology (CREST), FOCAS Institute, Dublin Institute of Technology, Dublin 8, Ireland

<sup>b</sup> School of Biological Sciences, Dublin Institute of Technology, Kevin Street, Dublin 8, Ireland

### ARTICLE INFO

#### Article history:

Received 30 September 2011  
Received in revised form  
12 December 2011  
Accepted 23 January 2012  
Available online xxx

#### Keywords:

Antibacterial activity  
Metal doped sol–gel  
Microtitre well coating

### ABSTRACT

The colonisation of clinical and industrial surfaces with microorganisms, including antibiotic-resistant strains, has promoted increased research into the development of effective antibacterial and antifouling coatings. This study describes the preparation of metal nitrate (Ag, Cu, Zn) doped methyltriethoxysilane (MTEOS) coatings and the rapid assessment of their antibacterial activity using polypropylene microtitre plates. Microtitre plate wells were coated with different volumes of liquid sol–gel and cured under various conditions. Curing parameters were analysed by thermogravimetric analysis (TGA) and visual examination. The optimum curing conditions were determined to be 50–70 °C using a volume of 200  $\mu$ l. The coated wells were challenged with Gram-positive and Gram-negative bacterial cultures, including biofilm-forming and antibiotic-resistant strains. The antibacterial activities of the metal doped sol–gel, at equivalent concentrations, were found to have the following order: silver > zinc > copper. The order is due to several factors, including the increased presence of silver nanoparticles at the sol–gel coating surface, as determined by X-ray photoelectron spectroscopy, leading to higher elution rates as measured by inductively coupled plasma atomic emission spectroscopy (ICP-AES). The use of microtitre plates enabled a variety of sol–gel coatings to be screened for their antibacterial activity against a wide range of bacteria in a relatively short time. The broad-spectrum antibacterial activity of the silver doped sol–gel showed its potential for use as a coating for biomaterials.

© 2012 Elsevier B.V. All rights reserved.

## 1. Introduction

Metals such as silver (Ag), gold (Au), copper (Cu) and zinc (Zn) are well known for their antibacterial activities [1] and are used for a number of *in vitro* and *in vivo* applications. Silver has been used to prevent bacterial colonisation of prostheses [2], catheters [3], and human skin [4]. In hospitals, copper alloys, used in doorknobs and other surfaces, exerted an *in vitro* antimicrobial effect against *Escherichia coli* O157, methicillin-resistant *Staphylococcus aureus* (MRSA) and *Clostridium difficile* while equivalent stainless steel surfaces did not [5–8]. Copper and zinc amalgams have proven useful in dental materials [6] while their salts have been incorporated into mouthwashes for the treatment of gingivitis [9].

The use of coatings with both low surface energies and antibacterial capabilities (*via* active additives) is an effective strategy for reducing microbial numbers on healthcare surfaces. The low surface energy chemistry minimises microbial attachment while antibacterial additives kill bacteria or inhibit their growth.

Moreover, these coatings can be engineered to release the active agents over a prolonged time period.

Antimicrobial agents (inorganic metal ions or organic molecules) can be incorporated into surface coatings by advanced deposition techniques such as vapour deposition, ion implantation, sputtering and electrochemical deposition from solution [10]. However, these technologies (a) can be costly, (b) are not easily applicable to large or complex items, (c) may not adhere sufficiently to the substrate without previous surface treatment and, (d) may lack transparency after application. A promising alternative technique for coating surfaces is the sol–gel method which requires low processing temperatures and produces a coating with high purity and homogeneity. Sol–gels are organic–inorganic hybrid polymers which produce glass-like surfaces with properties analogous to organic coatings. The sol–gel method offers a unique opportunity to incorporate metal components into a pure or organically modified inorganic matrix through a variety of methods such as entrapment, electrostatic interaction, adsorption and covalent binding [11].

In the present work, a coating strategy employing a combination of antibacterially active metal ions and hydrophobic chemistries to protect surfaces against the attachment of ionic precipitates and bacteria was investigated. The synthesis of silver, copper

\* Corresponding author. Tel.: +353 1 402 7964.  
E-mail address: [brendan.duffy@dit.ie](mailto:brendan.duffy@dit.ie) (B. Duffy).

and zinc ion doped methyltriethoxy silane (MTEOS) sol–gel, and their characterization by nuclear magnetic resonance (NMR) and thermogravimetric analysis (TGA) is described. A “microtitre well coating proliferation assay”, was used to evaluate the activities of these sol–gel coatings against a number of Gram-positive and Gram-negative bacteria and was found to be more rapid and less laborious than the standard JIS Z 2801 method. The surfaces of sol–gel coated glass slides were studied and compared using X-ray photoelectron spectroscopy (XPS) and contact angle analysis. The growth of biofilm-forming bacteria on the coated and uncoated glass slides was examined by scanning electron microscopy (SEM). Finally, the release rates of the different metal ions from the coated surfaces were studied and correlated with the efficacy data.

## 2. Experimental procedure

### 2.1. Preparation of metal doped methyltriethoxysilane (MTEOS) sol–gel

Methyltriethoxysilane (MTEOS) (Ger, Aldrich) was hydrolysed under acidic conditions in the presence of the metal nitrate salt of interest. All metal concentrations are presented in percentage (% w/w) relative to the final coating mass. To prepare stock MTEOS sol–gel, ethanol (17.5 ml) was added to precursor MTEOS (24 ml), followed by the gradual addition of nitric acid (3 ml of 0.04 M) and water (7.8 ml). This stock solution was stirred for 3 h and aliquoted (3 ml amounts) for doping purposes. Different doping concentrations [1, 0.7, 0.5, 0.3 and 0.1% (w/w)] of each of the metals (Ag, Cu, Zn) were achieved by direct addition of the corresponding metal nitrate [ $\text{AgNO}_3$ ,  $\text{Cu}(\text{NO}_3)_2 \cdot 2\text{H}_2\text{O}$  and  $\text{Zn}(\text{NO}_3)_2 \cdot 6\text{H}_2\text{O}$ ] (Aldrich) to the sol–gel solutions and stirred continuously for 24 h. A blank (metal free) sol–gel control was also prepared. Glassware containing silver nitrate dopants was wrapped with aluminium foil to prevent photo reduction of the silver ions.

### 2.2. Evaluation of sol–gel solutions

#### 2.2.1. Nuclear magnetic resonance (NMR) of metal doped sol–gel solutions

Chemical interaction between the silane matrix and the metal ions were analysed using liquid-state  $^{29}\text{Si}$  NMR spectroscopy using a Bruker 400 MHz spectrometer. The method determined the degree of hydrolysis and condensation of the organosilane skeleton structure in each system, as measured by the number of hydroxo and oxo bridges, respectively. Classical  $T$  notation was used for the different silicate species depending on the number of oxygen bridging atoms,  $i$  subscripts and  $j$  superscripts represent the number of hydroxo bridges and oxo functionalities respectively. The accumulation was carried out at a frequency of 79.49 MHz, with a pulse duration of 8 ms and a spectral width of 32,051 ppm for 30,000 scans. The chemical shifts were referenced against tetramethylsilane (TMS) as an external reference. Line broadening of 10 Hz was used for free induction decay processing. Each recorded spectrum is an average of all spectra obtained during the instrument acquisition time.

#### 2.2.2. Standardization of curing temperature by thermogravimetric analysis (TGA)

Optimum curing temperatures and times for the sol–gel were determined by TGA using a Shimadzu DTG 60 instrument. The experiment was carried out under a nitrogen flow of  $40 \text{ ml min}^{-1}$  at  $5^\circ\text{C}$  intervals between  $35$  and  $70^\circ\text{C}$  at a ramp rate of  $10^\circ\text{C min}^{-1}$  from ambient temperatures. Aluminium pans containing standard volumes of the different sol–gel samples were analysed at different time and temperature combinations. The shape and position of the peak maximum were related to the presence of solvent within the

sample and were, therefore, a reliable parameter for comparing the different sol–gel.

#### 2.2.3. Standardization of coating curing time and volume

The metal doped MTEOS sol–gels (50, 100, 150 and  $200 \mu\text{l}$  volumes) were dispensed into a 96-well microtitre plate and cured at the TGA-determined optimum temperature. Undoped MTEOS sol–gel was the control. The microtitre plate was examined visually after 8, 12, 24, 48, 72 and 96 h in the oven.

### 2.3. Physical evaluation of sol–gel coatings

Sol–gel solutions were spin coated onto pre-cleaned  $5 \text{ cm} \times 5 \text{ cm}$  glass slides at up to 1000 rpm, cured at  $70^\circ\text{C}$  for 24 h and stored at  $4^\circ\text{C}$  prior to XPS analysis, contact angle measurement and leaching studies.

#### 2.3.1. Surface study by XPS

Compositional XPS analysis of the sol–gel coating surfaces (top 10 nm) employed an ESCALAB Mk II spectrometer equipped with a twin anode X-ray source. The system consisted of a Vacuum Generator (VG) CLAM electron energy analyser operating at a pass energy of 20 eV, yielding an overall resolution of 1.2 eV. High voltage (10–15 keV) cathodes bombard the Mg and Al sources with high energy electrons thereby forcing X-rays to be emitted at peak intensities from the respective sources (Mg  $K\alpha = 1253.6 \text{ eV}$  and Al  $K\alpha = 1486.6 \text{ eV}$ ). All spectrum binding energies were referenced to the hydrocarbon C 1s peak at 285 eV to correct for electrostatic charging effects during acquisition. Sample mounting for XPS analysis was achieved by fixing a specimen to a VG sample stub using double sided adhesive tape (carbon pad sticker).

#### 2.3.2. Contact angle measurements

The wettability of the coated surface was estimated using a First Ten Angstroms (FTÅ, US) surface energy analyser. A water drop of defined volume was placed on the sample surface in the horizontal position. The drop formation and final shape were recorded with a high speed camera and the image processed by computer. Drop shape was evaluated in terms of the contact angle between the substrate surface and a tangent from the edge to the contour of the drop. Angles  $<90^\circ$  indicate a hydrophilic surface while values  $>90^\circ$  indicate a hydrophobic surface. All experiments were carried out in triplicate and the mean values reported.

#### 2.3.3. ICP-AES study of metal ion release rates

The release rate of the metal ions from the sol–gel coatings into sterile de-ionised water was analysed by ICP-AES (Varian Liberty 150). Plastic wells were attached to the surface of each sol–gel coating (1% of Ag, Cu and Zn) using an epoxy fixative (Araldite, Huntsman (UK)) and left for 24 h. Water (5 ml) was added to the wells and was removed and replaced with fresh water aliquots after 1, 4, 8, 12, 16, 20 and 24 h. All leachates were stored at  $4^\circ\text{C}$  prior to pooling and acidification with nitric acid (0.1 M) for analysis as a single batch by ICP-AES, using stock metal standard solutions for calibration purposes.

### 2.4. Antibacterial assay

#### 2.4.1. Bacterial strains and growth conditions

Bacterial strains used in this study included Gram-positive [*S. aureus* ATCC 25923 and *Staphylococcus epidermidis* CSF 41498, MRSA ATCC 43300], Gram-negative [*E. coli* ATCC 25922] and clinical isolates of multi-drug resistant (MDR) (ampicillin, gentamicin and ceftazidine) *Enterobacter Cloacae* WT6 and meropenem-resistant *Pseudomonas aeruginosa* WT2. These species are of public health

concern worldwide and are responsible for many healthcare-associated infections [12]. All cultures were grown, sub-cultured and maintained on Mueller-Hinton agar (LAB M) and stored at 4 °C. For the experiment, a single colony of each organism was inoculated into Mueller-Hinton broth (MHB, 10 ml) and incubated overnight (24 h) at 37 °C with shaking at 200 rpm. The optical density (OD) of the overnight culture was adjusted to that of a 0.5 McFarland standard ( $1.5 \times 10^8$  CFU ml<sup>-1</sup>) using a Densimat photometer (BioMerieux, France) and diluted with sterile MHB to give a final working concentration of  $1 \times 10^6$  CFU ml<sup>-1</sup>.

#### 2.4.2. Assessment of antibacterial activity of metal doped sol–gel coated microtitre wells

The antibacterial activity of the metal doped sol–gel coatings were assessed against the test organisms using a microtitre plate method [13]. Test bacteria (100 µl) from the  $10^6$  CFU ml<sup>-1</sup> suspensions were added to metal doped sol–gel coated wells. Control wells containing the respective cured metal doped MTEOS sol–gel with sterile MHB (100 µl) and the MTEOS undoped sol–gel with bacterial suspension (100 µl) were included in each assay. The microtitre plates were incubated for 24 h in a microtitre plate reader (Power-wave Microplate Spectrophotometer, Biotek, USA) at 37 °C.

#### 2.4.3. Determination of minimum incorporated inhibitory concentration (MIC) and minimum incorporated bactericidal concentration (MIBC)

The coating with the lowest metal concentration that completely inhibited bacterial growth after 24 h incubation at 37 °C was considered the MIC. The antibacterial activities of the different coatings were determined by calculating the percentage growth inhibition. MIBC was determined by the modified imprint method [14], where well contents (10 µl) were subcultured onto MHA plates. The MIBC was the lowest concentration that produced no visible bacterial growth on the MHA plate (after 24 h at 37 °C) indicating a 99.5% kill of the original inoculum. All experiments were performed in triplicate and repeated at least twice.

#### 2.4.4. Kinetic measurement of bacterial growth

Bacterial growth in the sol–gel coated wells was monitored by optical density measurements at 600 nm (OD<sub>600</sub>) over 24 h at 30 min intervals following a 30 s agitation step using the micro plate spectrophotometer. Growth curves of the test organisms were analysed graphically as a plot of OD<sub>600</sub> versus contact time.

#### 2.4.5. Biofilm growth on coated glass slide

The ability of metal-based coatings to prevent biofilm growth by *S. epidermidis* (CSF 41498) was assessed using scanning electron microscopy. Glass slides (1 cm<sup>2</sup>) were coated with the metal-doped or metal-free sol–gel and placed in a small Petri dish. *S. epidermidis* (5 ml of  $10^6$  CFU ml<sup>-1</sup> suspension) was added. After incubation of the dish for 3 days at 37 °C, the glass slides were removed, rinsed twice with sterile water, mounted on a stub and sputter coated with gold for SEM imaging at 12 KeV. Samples were kept at 4 °C prior to analysis.

## 3. Results and discussion

### 3.1. Metal doped sol–gel solution

#### 3.1.1. <sup>29</sup>Si Nuclear magnetic resonance (NMR) spectroscopy of metal doped sol–gel solution

The chemical interaction between metal dopants and the sol–gel matrix was analysed by <sup>29</sup>Si NMR to identify any structural variation in the sol–gel network formed. The NMR spectrum of the pure MTEOS precursor (Fig. 1) shows a single T<sub>0</sub><sup>0</sup> peak located at –44.03 ppm confirming the absence of any hydrolysed or modified

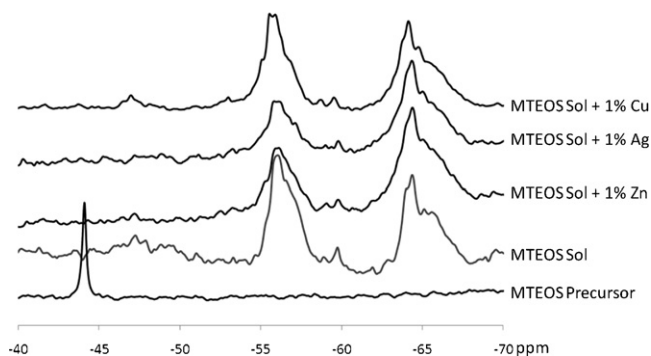


Fig. 1. NMR spectra of precursor-MTEOS, MTEOS sol, MTEOS sol with 1% Zn, MTEOS sol with 1% Ag, MTEOS sol with 1% Cu.

species. The control spectrum (MTEOS sol) shows the disappearance of the initial T<sub>0</sub><sup>0</sup> group observed in the precursor coupled with the appearance of 4 bands located around –47.22, –59.39, –55.83 and –64.35 ppm in the typical T<sub>1</sub><sup>0</sup>, T<sub>2</sub><sup>0</sup>, T<sub>2</sub><sup>1</sup> and T<sub>3</sub><sup>0</sup> regions respectively [15]. These bands are actually composed of several peaks indicating different degrees of hydrolysis for the silicon atom in each configuration, as summarised in Table 1. This demonstrates that the molecular system is composed of a mixture of oligomers of T<sub>1</sub>, T<sub>2</sub> and T<sub>3</sub>.

The Ag doped sol–gel solution spectrum indicates the presence of T<sub>2</sub><sup>1</sup> (–55.83) and T<sub>3</sub><sup>0</sup> (–64.35) species. The <sup>29</sup>Si NMR spectra of the corresponding MTEOS + Zn and MTEOS + Cu sol–gel show peaks similar to the MTEOS sol. Sol–gel formation is accompanied by an increase in siloxane bond signal, which was observed by an increase in T<sub>3</sub><sup>0</sup> species concentration and the disappearance of T<sub>2</sub><sup>1</sup> and T<sub>1</sub><sup>1</sup> species due to silanol groups.

Organic–inorganic hybrid material can be formed in two different ways, based on the type of bonds established between the organic and inorganic components. A network of both organic and inorganic compounds bonded through strong covalent or ion-covalent chemical bonds may be formed [16]. Alternatively organic molecules, oligomers or low molecular weight organic polymers may simply become embedded in the inorganic matrices. There were no significant differences between the spectra of the metal doped MTEOS sol–gel and the corresponding control (Fig. 1) which indicates they were primarily of the second type, although the relative T<sub>2</sub> signal intensities of the MTEOS + Ag and MTEOS + Zn peaks indicate the presence of some weak metal–silane interactions [17]. These results imply the metal species are entrapped within the silane matrix, with some weak chemical bonding in the case of silver and copper.

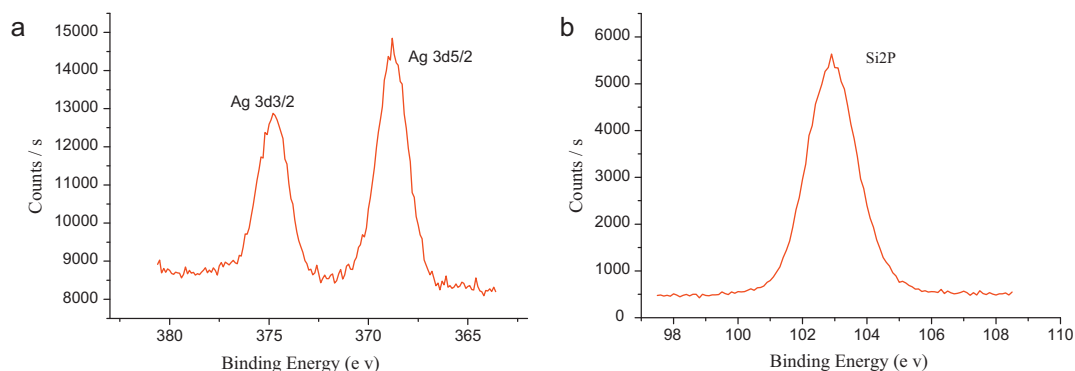
#### 3.1.2. Thermal analysis

Thermogravimetric analysis (TGA) is used to determine the sample weight change in a material in a controlled environment as a function of temperature and time. Synthesised organic–inorganic (sol–gel) suspensions contain large amounts of water and solvent. In the present study, TGA was used to estimate the optimum drying temperature of the sol–gel coatings.

There were weight losses after treatment at various temperatures over time. At the lower temperatures (35–40 °C) a gradual decrease in the weight loss was observed until 25 min whereas at higher temperatures (45–70 °C) full weight loss was achieved by 15 min. At the higher temperature the sol–gel dried faster than at the lower temperature and a thermal treatment of the gels at 50–70 °C was high enough to allow the evaporation of water, organic solvents and other moisture contents. Crucially this temperature range is below the softening (deformation) temperature of the polypropylene microtitre plates and, therefore, was chosen

**Table 1**  
Assignments of  $^{29}\text{Si}$  NMR signals for monomeric and oligomeric species obtained from the metal doped MTEOS sol–gel [15].

Silane structure	Notation	$i$	$j$	$k$	Chemical shift (ppm)
$(\text{OH})_j$	$T_0^0$	0	0	3	−44.03
$\text{Me}-\text{Si}-\text{(O-SiR}_3)_i$	$T_1^0$	1	0	2	−47.22
$(\text{OMe})_k$	$T_2^0$	2	0	1	−59.20
	$T_2^1$	2	1	0	−55.83
	$T_3^0$	3	0	0	−64.35

**Fig. 2.** XPS surface spectrum of (a) Ag 3d of silver-doped sol–gel and (b) Si 2p peak of methyl triethoxysilane (MTEOS) coating.

as the curing temperature of the sol–gel. However, since a full curing temperature can be in excess of  $100^\circ\text{C}$  complete condensation of the final silicate structure will not have occurred at  $50\text{--}70^\circ\text{C}$ . This means the coating is still porous and allows the release of the metal ions.

### 3.2. Metal-doped sol–gel film on glass slide

#### 3.2.1. Contact angle measurement on coated glass slides

The surface properties (hydrophobicity or hydrophilicity) of the coatings were analysed by contact angle measurements. In biological systems, the interaction between bacteria and surfaces is governed by hydrophobic interactions. Hydrophobic coatings may inhibit certain microbial interactions with the surface [18].

The contact angles of the sol–gel coated glass slides indicate that the metal doped surfaces were more hydrophobic when compared to the MTEOS control (Table 2). There was no discrimination between the contact angles of the different metal doped sol–gel coatings indicating no differences in hydrophobicity. This suggests that the increase in contact angle may be due to the common nitrate ion present, promoting a more dense surface structure.

#### 3.2.2. Surface study by XPS

The chemical state of the metals (Ag, Zn, and Cu) at the sol–gel coated glass slide surface was analysed by XPS. This is a useful analytical tool in bioengineering for determining the chemical state of specific functional groups in the uppermost 10 nm of a surface coating [19]. The presence of silver in the surface coating was confirmed by the presence of the peak at  $368.2\text{ eV}$  indicative of  $\text{Ag}^0$ ,

**Table 2**  
Contact angle of MTEOS (Control) and Ag, Zn and Cu doped sol–gel coatings.

Sol–gel coating	Contact angle
MTEOS (control)	$90.34^\circ$
Ag–MTEOS	$104.53^\circ$
Zn–MTEOS	$102.35^\circ$
Cu–MTEOS	$103.78^\circ$

most likely in a nanoparticle form (Fig. 2a) [20]. Due to the low curing temperature used and the absence of the characteristic yellow (plasmon induced) colour, it is likely that the nanoparticles are below 50 nm in size. This agrees with previous work on silver doped phenyltriethoxy silane (PhTEOS) sol–gel coatings [21]. In contrast the respective signature peaks for zinc and copper were not detected suggesting they may be in their oxide form, CuO and ZnO respectively. As expected peaks corresponding to the Si 2p electrons with binding energies of  $102.8\text{ eV}$  were observed (Fig. 2b). This is consistent with previous reports on silver-doped silica films, indicating ionic network formation analogous to soda glass [22].

#### 3.2.3. Evaluation of metal ion release rate

For coatings on biomedical devices, high initial release rates of antibacterial agents are desirable to deter biofilm establishment. Previous studies have shown that when silver salts are incorporated into sol–gel coatings a high initial release of silver ions is followed by a more gradual and sustained release profile [19]. Ion release from such biomaterials is governed by (a) the amount of available surface metal, (b) the area of the exposed coating, (c) the degree of hydrophobicity of the coating inter–face, and (d) the volume of the contact fluid [23]. The release of silver, copper and zinc at 1% (w/w) loadings into de-ionised water over a 24 h period at  $37^\circ\text{C}$  is presented in Fig. 3. During the first hour, approximately 50, 35 and  $28\text{ ppm m}^{-2}$  of  $\text{Ag}^+$ ,  $\text{Zn}^{2+}$  and  $\text{Cu}^{2+}$  ions were released respectively. This was followed by a lower sustained release profile for 24 h (6 exposure cycles), indicating that antibacterial activity can be maintained after repeated challenges. The variability between elution profiles is probably due to the chemical state of the metals in the coatings. As the silver is most likely in nanoparticulate form, its release would be more rapid than that of copper and zinc in their more stable oxide forms. An initial high release of a broad spectrum antibacterial agent is desirable (Fig. 4) as the first 6 h after device implantation is critical in bacterial colonisation.

Low temperature processing maintains silver in the upper (surface) regions of the sol–gel derived coatings, enhancing the release of biocidal silver ions into the surrounding medium [21]. High

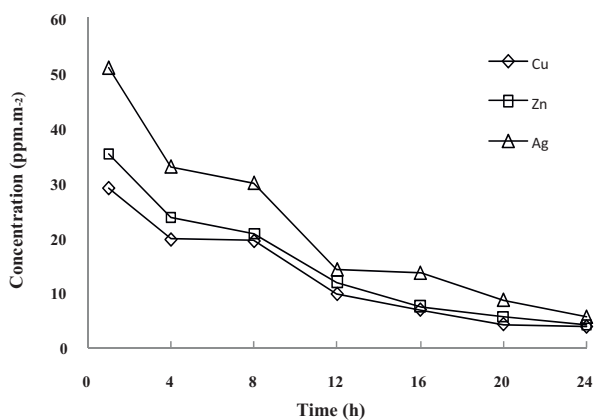


**Fig. 3.** Non-cumulative release rates of Ag, Zn and Cu into fresh DiH<sub>2</sub>O from Ag:MTEOS, Zn:MTEOS, Cu:MTEOS coatings (determined by ICP emission spectrometer).

temperature processing of silver doped sol–gel systems can lead to diffusion of silver away from the surface into the coating bulk.

### 3.3. Antibacterial assay

#### 3.3.1. Microtitre well coated proliferation assay

The antibacterial activities (MIICs and MIBCs) of the coatings (blank, Ag<sup>+</sup>, Zn<sup>2+</sup> and Cu<sup>2+</sup>) against Gram-positive and Gram-negative bacteria were determined (Table 3). The MIIC for the Ag<sup>+</sup> coating against *P. aeruginosa* WT2, *Enterobacter* WT6 and *E. coli* was 0.5% (w/w). The MIBC results were identical. In contrast, the MIICs of the Cu<sup>2+</sup> coatings were lower than those of Zn<sup>2+</sup> against the Gram-negative bacteria tested (Table 2). MIIC values against Gram-positive, *S. aureus* and MRSA, displayed a similar trend, namely Ag > Zn > Cu. Generally, the MIBC and MIIC for each tested strain was the same.

**3.3.1.1. Time dependent study.** Fig. 4 shows the time dependent inhibitory effect of the various coatings (0.7, 0.5 and 0.3% (w/w)

of Ag<sup>+</sup>, Cu<sup>2+</sup> and Zn<sup>2+</sup> respectively) on *E. coli* and *S. aureus*. Bacteria in the control wells, coated with the undoped sol–gel showed a rapid growth with a short lag phase of 2 h. The incorporation of different metal concentrations resulted in variable levels of inhibition in bacterial growth resulting in prolonged lag phases and lower overall growth at 24 h. *E. coli* had the longest lag phase (15 h) in the Ag<sup>+</sup> coated wells followed by Zn<sup>2+</sup> (5 h) and Cu<sup>2+</sup> (4 h) at sub MIIC values (0.3%, 0.5%, 0.5% (w/w) respectively).

In the case of Gram-positive bacteria *S. aureus* at the lower dose of 0.3% (w/w), there was no growth and therefore no lag phase for Ag<sup>+</sup>, while Zn<sup>2+</sup> and Cu<sup>2+</sup> delayed growth for 10 and 5 h at sub MIIC values of 0.5% and 0.7% (w/w) respectively. The antibacterial properties of the metal doped sol–gel layer on the microtitre well surfaces may be attributed to the mutual attraction, potentially via electrostatic forces, of the negatively charged bacteria to the siloxane surface, where the positive charged metal ions released kill the bacteria or hinder their replication mechanisms [24]. The results showed the Ag<sup>+</sup> doped sol–gel coatings to have a consistently higher antibacterial activity against all the test bacteria followed by Zn<sup>2+</sup> and Cu<sup>2+</sup>. The higher killing rate of the Ag<sup>+</sup> sol–gel coating is due to a combination of a greater potency and a higher release of the ion from the enriched surface, as proven by the XPS data. Silver doped materials can be chemically durable and release silver ions over extended periods of time [25]. In combination with the higher efficacy of Ag<sup>+</sup> and the surface enrichment, it is important to note that the lower loading levels were still more effective than the higher Zn<sup>2+</sup> and Cu<sup>2+</sup> equivalents.

#### 3.3.2. Biofilm growth on coated glass slide

In biomedical and implant-device coatings, the biomaterial surface chemistry is a key factor that influences initial bacterial attachment. Biofilm formation is a multi-factorial process involving the adhesion of bacterial cells to a host substrate, followed by multiplication. *S. epidermidis* is the most frequently isolated bacterium from implant device-related infections, as it colonises surfaces resulting in biofilm formation [26]. Silver ions have recently been reported to destabilise biofilms [27]. Silver-impregnated catheters have demonstrated superior inhibition of bacterial colonisation than antibiotic-impregnated catheters [28].

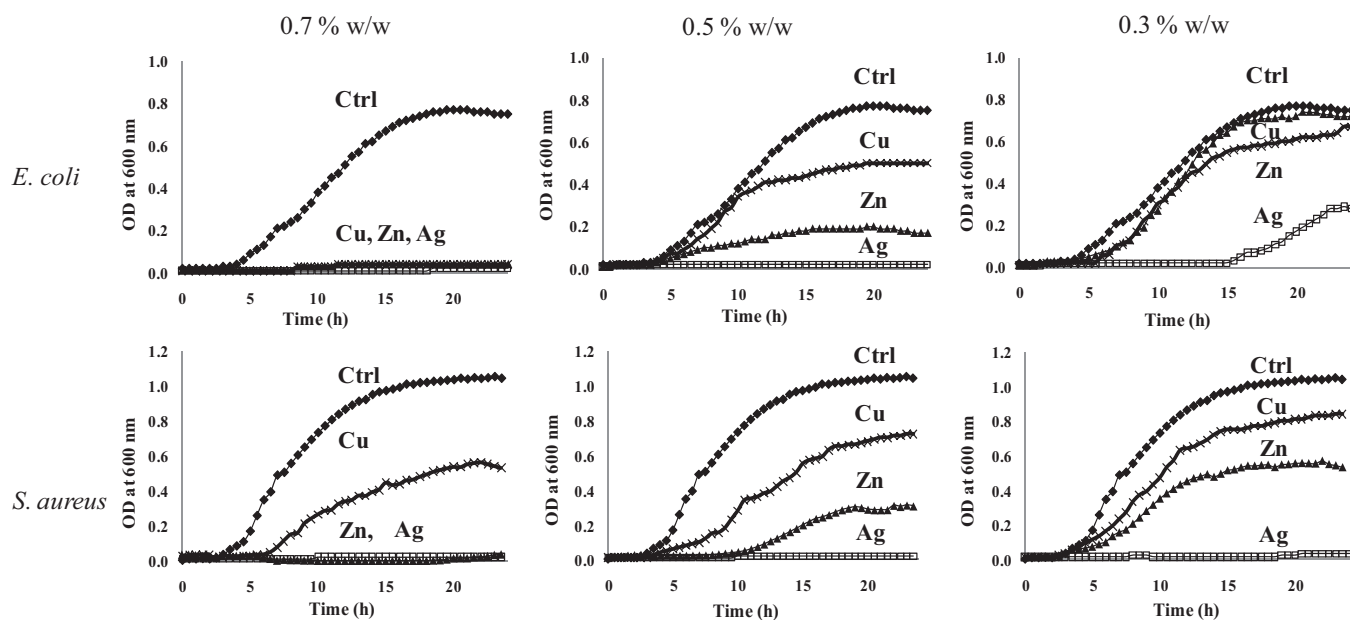


**Fig. 4.** Comparative growth curves of Gram negative *E. coli* ATCC 25922 and Gram positive *S. aureus* ATCC 25923 on the coated sol–gel microtitre well surface containing metal ions (Ag (—■—), Zn (—▲—), Cu (—◆—)) of different concentrations (a) 0.7% (w/v), (b) 0.5% (w/v) and (c) 0.3% (w/v) with respect to control (—●—) (MTEOS coated surface without metal ions) after 24 h of incubation.

**Table 3**  
Minimum inhibitory concentrations (MIC) and minimum bactericidal concentrations (MBC) of different concentrations (0.3%, 0.5%, 0.7% and 1.0%, w/w) of metal doped sol–gel (Ag–MTEOS, Zn–MTEOS and Cu–MTEOS) against Gram-positive and Gram-negative bacteria.

	Samples (metal doped sol–gel)	Organisms	MIC (% w/w)	MBC (% w/w)
Gram-positive	Ag	<i>S. aureus</i> ATCC 25923	0.5	0.5
	Zn		0.7	0.7
	Cu		>1	>1
	Ag	<i>S. epidermidis</i> CSF 41498	0.7	0.7
	Zn		1	1
	Cu		1	1
	Ag	MRSA ATCC 43300	0.3	0.7
	Zn		>1	>1
	Cu		>1	>1
	Gram-negative	Ag	Meropenem resistant <i>P. aeruginosa</i> WT2	0.5
Zn		0.7		1
Cu		>1		>1
Ag		Multi drug resistant <i>Enterobacter</i> WT6	0.5	0.3
Zn			1	1
Cu			>1	>1
Ag		<i>E. coli</i> ATCC 25922	0.5	0.5
Zn			0.7	0.7
Cu			0.7	0.7

The antibacterial effect of metal ion release on the sol–gel surface is shown in the SEM images in Fig. 5. After exposure to *S. epidermidis* the blank undoped MTEOS-coated glass slides were covered in adherent bacterial deposits, with fully formed bacteria observed (Fig. 5a). Silver ion release from the silver doped MTEOS (Fig. 5b) reduced colonisation of the coating. There was evidence of bacterial lysis. A similar effect was observed for microbial deposits on the zinc doped coatings (Fig. 5c), while some bacterial colonisation was observed on the copper doped coatings (Fig. 5d).

The broad spectrum antibacterial activity of these metal coatings suggests they would be useful in preventing environmental contamination on surfaces such as door plates and handles, light switches, and hand and bedside rails in healthcare environments. This is important as patients and staff colonised or infected with healthcare and community associated microorganisms may transfer them onto such fomites found in hospitals, nursing homes, childcare facilities, prisons and public transport [29]. Additionally as silver ion release is governed by water diffusion through the coating [30] then the use of water alone as a cleaning agent, in the

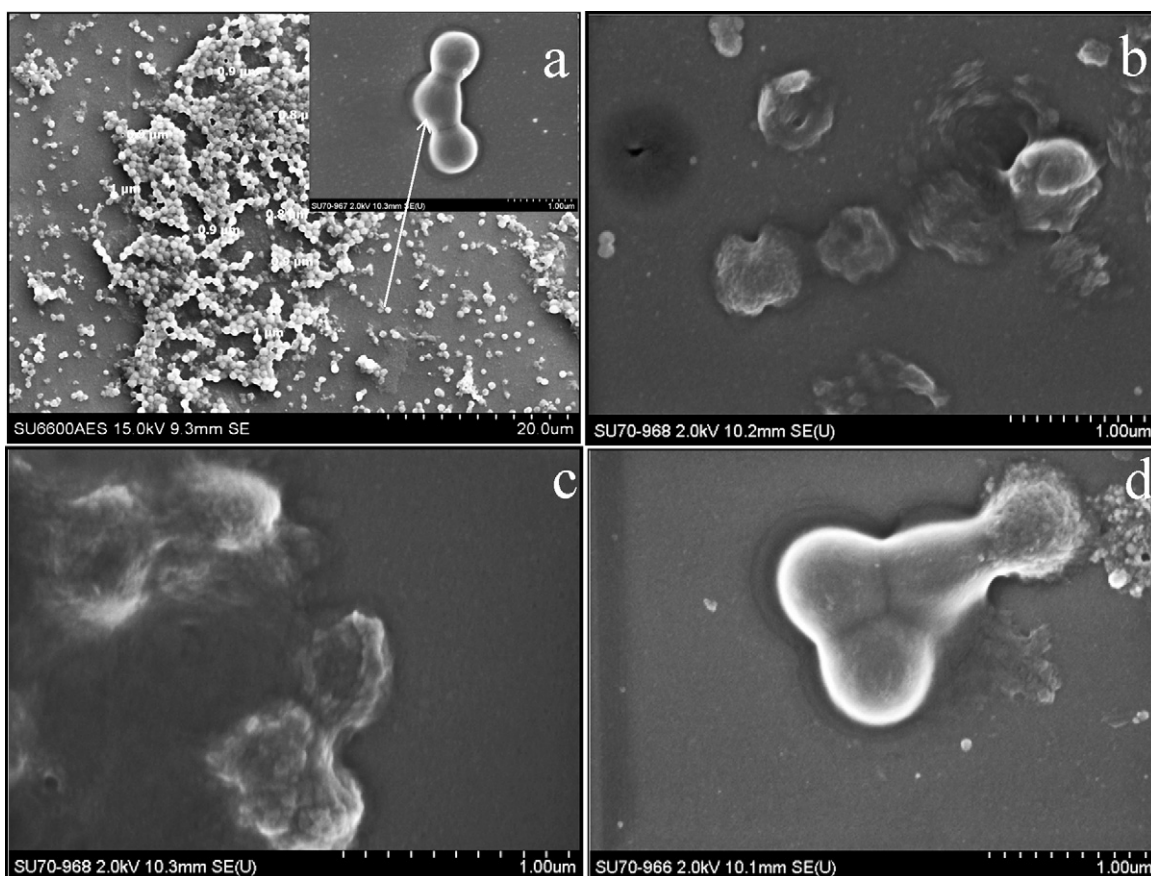


**Fig. 5.** SEM images of *S. epidermidis* CSF41498 on (a) MTEOS coated glass slide without metals, (b) Ag–MTEOS coated glass slide, (c) Zn–MTEOS coated glass slides and (d) Cu–MTEOS coated glass slides, with all MIBC level of metals.

absence of standard antiseptics and detergents, may be sufficient to generate enhanced bioactive surfaces.

#### 4. Conclusion

The increasing incidence the healthcare-associated antibiotic-resistant pathogens has stimulated the search for novel agents to combat them. A method to rapidly assess the activity of antibacterial agent-impregnated coated surfaces against a number of organisms is demonstrated here. The microtitre well coating method is less laborious and more cost effective than conventional methods. It was used for preliminary antibacterial screening of different concentrations of metal ion ( $\text{Ag}^+$ ,  $\text{Zn}^{2+}$ , and  $\text{Cu}^{2+}$ ) doped sol–gel. The release rates and antibacterial activities of the doped sol–gel were in the order of  $\text{Ag}^+ > \text{Zn}^{2+} > \text{Cu}^{2+}$ . XPS measurements confirmed the presence of surface Ag whereas no detectable levels of Zn and Cu were observed on the corresponding coated glass slide surface. The release of  $\text{Ag}^+$  from the sol–gel coating inhibited the development of a *S. epidermidis* biofilm over a 72 h period. As the first 6 h are considered critical after device insertion, an initial high release of  $\text{Ag}^+$  compared to  $\text{Zn}^{2+}$  and  $\text{Cu}^{2+}$  is beneficial for reducing bacterial adhesion. The results of this work indicate that silver release coatings are more suitable for the protection of various surfaces against bacterial infection than zinc and copper equivalents.

#### Acknowledgements

The authors would like to gratefully acknowledge Dr. Rosaria Leyden, Ms. Emer Ryan and Ms Aisling Kirwan. The authors would also like to acknowledge the Dublin Institute of Technology, Dublin, Ireland for funding under the ABBEST scholarship programme.

#### References

- [1] A.M. Schrand, M.F. Rahman, S.M. Hussain, J.J. Schlager, D.A. Smith, A.F. Syed, *Nanomed. Nanobiotechnol.* 2 (2010) 544–568.
- [2] G. Gosheger, J. Harges, H. Ahrens, A. Streitburger, H. Buerger, M. Erren, A. Gonsel, F.H. Kemper, W. Winkelmann, C. Von Eiff, *Biomaterials* 25 (2004) 5547–5556.
- [3] M.E. Rupp, T. Fitzgerald, N. Marion, V. Helget, S. Puumala, J.R. Anderson, P.D. Fey, *Am. J. Infect. Control* 32 (2004) 445–450.
- [4] H.J. Lee, S.H. Jeong, *Text. Res. J.* 75 (2005) 551–556.
- [5] G. Grass, C. Rensing, M. Solioz, *Appl. Environ. Microbiol.* 77 (2011) 1541–1547.
- [6] C.E. Santo, N. Taudte, D.H. Nies, G. Grass, *Appl. Environ. Microbiol.* 74 (2008) 977–986.
- [7] S.A. Wilks, H. Michels, C.W. Keevil, *Int. J. Food Microbiol.* 105 (2005) 445–454.
- [8] J.O. Noyce, H. Michels, C.W. Keevil, *J. Hosp. Infect.* 63 (2006) 289–297.
- [9] J.J. Morrier, G. Suchett-Kaye, D. Nguyen, J.P. Rocca, J. Blanc-Benon, O. Barsotti, *Dent. Mater.* 14 (1998) 150–157.
- [10] J.E. Gray, P.R. Norton, R. Alnouno, C.L. Marolda, M.A. Valvano, K. Griffiths, *Biomaterials* 24 (2003) 2759–2765.
- [11] M. Marini, M. Bondi, R. Iseppi, M. Toselli, F. Pilati, *Eur. Polym. J.* 43 (2007) 3621–3628.
- [12] Y. Li, P. Leung, L. Yao, Q.W. Song, E. Newton, *J. Hosp. Infect.* 62 (2006) 58–63.
- [13] S. Jaiswal, B. Duffy, A.K. Jaiswal, N. Stobie, P. McHale, *Int. J. Antimicrob. Agents* 36 (2010) 280–283.
- [14] A. Panáček, L. Kvítek, R. Prucek, M. Kolář, R. Večeřová, N. Pizúrová, V.K. Sharma, T. Nevečna, R. Zboril, *J. Phys. Chem. B* 110 (2006) 16248–16253.
- [15] A. Jitianu, A. Britchi, C. Deleanu, V. Badescu, M. Zaharescu, *J. Non-Cryst. Solids* 319 (2003) 263–279.
- [16] C. Sanchez, G.J.d.A.A. Soler-Illia, F. Ribot, T. Lalot, C.R. Mayer, V. Cabuil, *Chem. Mater.* 13 (2001) 3061–3083.
- [17] K.H. Wu, C.I. Liu, C.C. Yang, G.P. Wang, C.M. Chao, *Mater. Chem. Phys.* 125 (2011) 802–806.
- [18] N. Cerca, G.B. Pier, M. Vilanova, R. Oliveira, J. Azeredo, *Res. Microbiol.* 156 (2005) 506–514.
- [19] N. Stobie, B. Duffy, S.J. Hinder, P. McHale, D.E. McCormack, *Colloids Surf. B* 72 (2009) 62–67.
- [20] W. Li, S. Seal, E. Megan, J. Ramsdell, K. Scammon, G. Lelong, L. Lachal, K.A. Richardson, *J. Appl. Phys.* 93 (2003) 9553–9561.
- [21] N. Stobie, B. Duffy, D.E. McCormack, J. Colreavy, M. Hidalgo, P. McHale, S.J. Hinder, *Biomaterials* 29 (2008) 963–969.
- [22] A. Babapour, O. Akhavan, R. Azimirad, A.Z. Moshfeghi, *Nanotechnology* 17 (2006) 763–771.
- [23] E.M. Hetrick, M.H. Schoenfish, *Chem. Soc. Rev.* 35 (2006) 780–789.
- [24] V. Sambhy, M.M. MacBride, B.R. Peterson, A. Sen, *J. Am. Chem. Soc.* 128 (2006) 9798–9808.
- [25] F. Furno, K.S. Morley, B. Wong, B.L. Sharp, P.L. Arnold, S.M. Howdle, R. Bayston, P.D. Brown, P.D. Winship, H.J. Reid, *J. Antimicrob. Chemother.* 54 (2004) 1019–1024.
- [26] D. Roe, B. Karandikar, N. Bonn-Savage, B. Gibbins, J.-B. Rouillet, *J. Antimicrob. Chemother.* 61 (2008) 869–876.
- [27] N. Stobie, B. Duffy, J. Colreavy, P. McHale, S.J. Hinder, D.E. McCormack, *J. Colloid Interface Sci.* 345 (2010) 286–292.
- [28] K. Galiano, C. Pleifer, K. Engelhardt, G. Brössner, P. Lackner, C. Huck, C. Lass-Flörl, A. Obwegeser, *Neurol. Res.* 30 (2008) 285–287.
- [29] B. Eckstein, D. Adams, E. Eckstein, A. Rao, A. Sethi, G. Yadavalli, C. Donskey, *BMC Infect. Dis.* 7 (2007) 61–66.
- [30] R. Kumar, H. Münstedt, *Polym. Int.* 54 (2005) 1180–1186.